Cite this: *CrystEngComm*, 2012, **14**, 3456

www.rsc.org/crystengcomm

PAPER

Near-infrared (NIR) luminescent homoleptic lanthanide Salen complexes $Ln_4(Salen)_4$ (Ln = Nd, Yb or Er)†

Weixu Feng,[a] Yao Zhang,[a] Xingqiang Lü,*[ab] Yani Hui,[a] Guoxiang Shi,[a] Dan Zou,[a] Jirong Song,[a] Daidi Fan,[a] Wai-Kwok Wong*[c] and Richard A. Jones[d]

Received 23rd November 2011, Accepted 2nd March 2012
DOI: 10.1039/c2ce06566e

The series of homoleptic tetranuclear $[Ln_4(L)_2(HL)_2(NO_3)_2(OH)_2]\cdot 2(NO_3)$ (Ln = Nd, **1**; Ln = Yb, **2**; Ln = Er, **3**; Ln = Gd, **4**) have been self-assembled from the reaction of the Salen-type Schiff-base ligand $\mathbf{H_2L}$ with $Ln(NO_3)_3\cdot 6H_2O$ (Ln = Nd, Yb, Er or Gd), respectively ($\mathbf{H_2L}$: *N*,*N*′-bis(salicylidene) cyclohexane-1,2-diamine). The result of their photophysical properties shows that the strong and characteristic NIR luminescence for complexes **1** and **2** with emissive lifetimes in microsecond ranges are observed and the sensitization arises from the excited state (both ^{1}LC and ^{3}LC) of the Salen-type Schiff-base ligand with the flexible linker.

1. Introduction

Recent startling interest for polynuclear Ln^{3+} complexes with the unusual photophysical and magnetic properties, is stimulated by the continuously expanding need for luminescent[1] and magnetic materials.[2] However, the synthesis is often problematic due to the high coordination numbers and the flexible coordination geometries adopted by the Ln^{3+} ions.[3] In fact, the challenge to resolve the problem is strengthened because the construction of the polynuclear Ln^{3+} complexes is distinctively affected by a variety of factors, such as the character of organic ligands,[4] the nature of counter anions[5] and the reaction conditions.[6] From the viewpoint of self-assembly of the polynuclear Ln^{3+} complexes with good photophysical properties, this requires that the strong light-harvesting of the organic chromophores, the effective energy transfer from the chromophores to the Ln^{3+} ions and the minimization of non-radiative processes of the Ln^{3+} are achieved,[7] besides completely avoiding or decreasing the luminescent quenching effect arising from OH-, CH- or NH-oscillators around the Ln^{3+} ion.[8]

Compared to the amount of effort on the photophysical behavior of 3d–4f heteronuclear complexes from compartmental Salen-type Schiff-base ligands,[9] the photophysical properties of polynuclear lanthanide Salen complexes have not been researched nearly as extensively, especially the limited single-crystal X-ray diffraction study has been reported for those classic complexes.[10] Nonetheless, in the formation of the series of binuclear triple-decker,[11] trinuclear triple-decker,[12] trinuclear tetra-decker[13] or pentanuclear tetra-decker lanthanide complexes,[14] different Salen-type Schiff-base ligands with rigid linkers have been used, and their photophysical properties should be further enhanced, despite the chromophores with rigid linkers absorbing at longer wavelength. Moreover, the self-assembly from LnX_3 ($X^- = OAc^-$ or $CF_3SO_3^-$) with the Salen-type Schiff-base ligands with the flexible linkers usually gives the formation of polymeric lanthanide coordination complexes, not the discrete polynuclear lanthanide complexes.[15] In particular, the recent report of discrete binuclear or tetranuclear homoleptic lanthanide Salen complexes[16] revealed that the pure Salen-type Schiff-base ligand without the outer O_2O_2 moiety could coordinate with the Ln^{3+} ions in quadridentate and bidentate modes, while the self-assembly process is complicated, anion-dependent and strictly relative to the detailed reaction conditions. To the best of our knowledge, no report of the self-assembly of polynuclear lanthanide complexes from flexible hexadentate Salen-type Schiff-base ligands with the outer O_2O_2 moiety has been documented. Herein, starting from the Salen-type Schiff-base ligand $\mathbf{H_2L}$ ($\mathbf{H_2L}$ = *N*,*N*′-bis(3-methoxy-salicylidene)cyclohexane-1,2-diamine) with the flexible linker, the richness of its coordination modes ($\mathbf{(L)^{2-}}$ and $\mathbf{(HL)^-}$ modes, as shown in Scheme 1) endows the formation of series of homoleptic tetranuclear $[Ln_4(L)_2(HL)_2(NO_3)_2(OH)_2]\cdot 2(NO_3)$ (Ln = Nd, **1**; Ln = Yb, **2**; Ln = Er, **3**; Ln = Gd, **4**) under similar reaction conditions. The sensitization and the energy transfer for the NIR luminescence of the Ln^{3+} ions in the homoleptic tetranuclear $Ln_4(Salen)_4$ complexes are discussed.

[a]*Shaanxi Key Laboratory of Degradable Medical Material, Shaanxi Key Laboratory of Physico-inorganic Chemistry, Northwest University, Xi'an 710069, Shaanxi, China. E-mail: lvxq@nwu.edu.cn*
[b]*Fujian Institute of Research on the Structure of Matter, Chinese Academy of Science, Fuzhou 350002, Fujian, China*
[c]*Department of Chemistry, Hong Kong Baptist University, Waterloo Road, Kowloon Tong, Hong Kong, China. E-mail: wkwong@hkbu.edu.hk*
[d]*Department of Chemistry and Biochemistry, The University of Texas at Austin, 1 University Station A5300, Austin, TX 78712-0165, United States*
† Electronic supplementary information (ESI) available. CCDC reference numbers 854306–854308. For ESI and crystallographic data in CIF or other electronic format see DOI: 10.1039/c2ce06566e

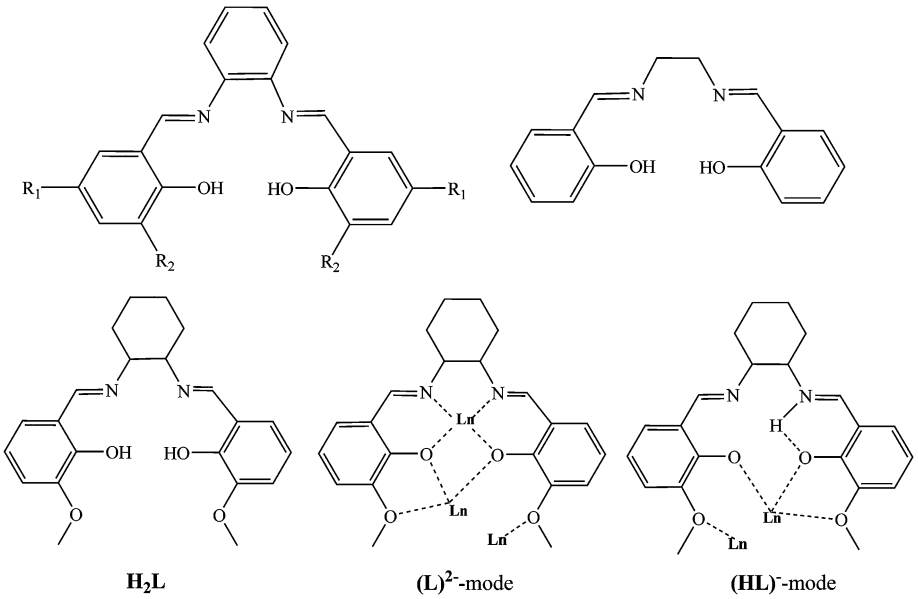

Scheme 1 Molecular structures and bonding modes of Salen-type Schiff-base ligands for polynuclear or polymeric lanthanide complexes.

2. Experimental

All chemicals were commercial products of reagent grade and were used without further purification. Elemental analyses were performed on a Perkin-Elmer 240C elemental analyzer. Infrared spectra were recorded on a Nicolet Nagna-IR 550 spectrophotometer in the region 4000–400 cm^{-1} using KBr pellets. ^1H NMR spectra were recorded on a JEOL EX270 spectrometer with $SiMe_4$ as internal standard in CD_3CN at room temperature. ESI-MS was performed on a Finnigan LCQ^{DECA} XP HPLC-MS_n mass spectrometer with a mass to charge (*m*/*z*) range of 4000 using a standard electrospray ion source and MeCN or MeOH as solvent. Electronic absorption spectra in the UV/Vis region were recorded with a Cary 300 UV spectrophotometer, and steady-state visible fluorescence, PL excitation spectra on a Photon Technology International (PTI) Alphascan spectrofluorometer and visible decay spectra on a pico-N_2 laser system (PTI Time Master). The quantum yield of the visible luminescence for each sample was determined by the relative comparison procedure, using a reference of a known quantum yield (quinine sulfate in dilute H_2SO_4 solution, $\Phi_{em} = 0.546$). NIR emission and excitation in solution were recorded by PTI QM4 spectrofluorometer with a PTI QM4 Near-Infrared InGaAs detector.

Syntheses

H_2L (H_2L: *N*,*N*′-bis(3-methoxy-salicylidene)cyclohexane-1,2-diamine). To a stirred solution of an equimolar mixture of *cis*- and *trans*-1,2-diaminocyclohexane (6.0 mL, 50 mmol) in absolute EtOH (20 mL), *o*-vanillin (15.0 g, 100 mmol) was added, and the resulting mixture was refluxed for 5 h. After cooling to room temperature, the insoluble yellow precipitate was filtered and was recrystallized using absolute EtOH to give a pale yellow polycrystalline solid. Yield: 13.6 g, 71%. Calc. for $C_{22}H_{26}N_2O_4$: C 69.09, H 6.85, N 7.32%; found: C, 69.01, H, 6.94, N, 7.26%. IR (KBr, cm^{-1}): 3455 (b), 3058 (w), 2933 (w), 2862 (w), 2597 (w), 1619 (s), 1588 (w), 1470 (s), 1418 (m), 1345 (w), 1251 (vs), 1196 (w), 1168 (w), 1144 (w), 1085 (m), 1036 (w), 984 (m), 953 (w), 894 (w), 849 (m), 776 (w), 731 (m), 668 (w), 616 (w), 595 (w), 568 (w), 516 (w), 467 (w), 422 (w). ^1H NMR (400 MHz, CD_3CN): δ (ppm) 13.84 (s, 2H, –OH), 8.24 (s, 2H, –CH=N), 6.85 (d, 2H, –Ph), 6.78 (d, 2H, –Ph), 6.72 (t, 2H, –Ph), 3.86 (s, 6H, MeO–), 3.32 (m, 2H, –Ch), 1.92 (m, 4H, –Ch), 1.58 (m, 4H, –Ch).

Synthesis of $[Nd_4(L)_2(HL)_2(NO_3)_2(OH)_2]\cdot 2(NO_3)$ (1). To a stirred solution of **H_2L** (0.115 g, 0.3 mmol) in absolute MeCN (10 mL), Et_3N (100 μL) and a solution of $Nd(NO_3)_3\cdot 6H_2O$ (0.3 mmol, 0.117 g) in absolute MeOH (10 mL) were added, respectively. The resultant mixture was refluxed for 2 h, and the clear pale yellow solution was then cooled to room temperature and filtered. Diethyl ether was allowed to diffuse slowly into the filtrate at room temperature and the pale yellow microcrystal products of **1** were obtained in a few weeks. For **1**: Yield: 0.118 g, 67%. Anal. Calc. for $C_{88}H_{100}N_{12}O_{30}Nd_4$: C, 44.36; H, 4.23; N, 7.05%; found: C, 44.15; H, 4.37; N, 7.01%. IR (KBr, cm^{-1}): 3402 (b), 3065 (w), 2938 (m), 2857 (w), 1648 (s), 1615 (m), 1556 (m), 1503 (m), 1452 (vs), 1384 (m), 1355 (w), 1283 (s), 1237 (w), 1221 (s), 1169 (m), 1144 (w), 1098 (w), 1075 (m), 1058 (w), 1019 (w), 946 (w), 902 (w), 847 (m), 783 (w), 742 (m), 659 (w), 605 (w), 561 (w), 491 (w), 470 (w), 433 (w). ^1H NMR (400 MHz, CD_3CN): δ (ppm) 14.58 (s, 4H), 14.17 (s, 4H), 10.10 (t, 4H), 9.40 (t, 4H), 8.61 (d, 4H), 8.36 (d, 4H), 7.59 (m, 4H), 6.53 (m, 4H), 5.48 (m, 12H), 4.66 (m, 12H), 4.02 (m, 4H), 3.80 (m, 4H), 1.70 (s, 6H), 1.31 (s, 6H), 1.16 (m, 3H), 1.03 (m, 3H), −0.10 (m, 4H), −0.42 (m, 4H), −0.81 (m, 4H), −1.23(m, 4H), −1.83 (m, 4H), −2.65(m, 4H), −2.90 (m, 4H), −5.68 (m, 4H). ESI-MS (in MeCN) *m*/*z*: 2320.78 (100%), $[M - NO_3]^+$; 1129.38 (45%), $[M - (NO_3)_2]^{2+}$; 745.94 (4%), $[M - (NO_3)_3 + (MeCN)]^{3+}$ and 554.22 (11%), $[M - (NO_3)_4 + (MeCN)_2]^{4+}$; ESI-MS (in MeOH) *m*/*z*: 2320.78 (100%), $[M - NO_3]^+$; 1129.38 (41%), $[M - (NO_3)_2]^{2+}$, 742.94 (5%), $[M - (NO_3)_3 + (MeOH)]^{3+}$ and 549.71 (10%), $[M - (NO_3)_4 + (MeOH)_2]^{4+}$.

Synthesis of $[Yb_4(L)_2(HL)_2(NO_3)_2(OH)_2]\cdot 2(NO_3)$ (2). The complex **2** was prepared in the same way as **1** except that $Yb(NO_3)_3\cdot 6H_2O$ (0.3 mmol, 0.126 g) was used instead of $Nd(NO_3)_3\cdot 6H_2O$ (0.3 mmol, 0.117 g). For **2**: Yield: 0.109 g, 58%. Anal. Calc. for $C_{88}H_{100}N_{12}O_{30}Yb_4$: C, 42.31; H, 4.04; N, 6.73%; found: C, 42.18; H, 4.17; N, 6.66%. IR (KBr, cm^{-1}): 3411 (b), 3065 (w), 2936 (m), 2861 (w), 1653 (s), 1618 (m), 1560 (m), 1505 (m), 1476 (vs), 1384 (m), 1360 (w), 1291 (s), 1236 (w), 1229 (s), 1168 (m), 1143 (w), 1100 (w), 1078 (m), 1060 (w), 1042 (w), 1022 (w), 949 (w), 903 (w), 847 (m), 782 (w), 738 (m), 695 (w), 660 (w), 613 (w), 561 (w), 502 (w), 482 (w), 448 (w). ESI-MS (in MeCN) *m/z*: 2435.98 (100%), $[M - NO_3]^+$; 1186.98 (41%), $[M - (NO_3)_2]^{2+}$; 784.34 (6%), $[M - (NO_3)_3 + (MeCN)]^{3+}$ and 583.02 (13%), $[M - (NO_3)_4 + (MeCN)_2]^{4+}$; ESI-MS (in MeOH) *m/z*: 2435.98 (100%), $[M - NO_3]^+$; 1186.98 (40%), $[M - (NO_3)_2]^{2+}$; 748.00 (8%), $[M - (NO_3)_3 + (MeOH)]^{3+}$ and 578.51 (14%), $[M - (NO_3)_4 + (MeOH)_2]^{4+}$.

Synthesis of $[Er_4(L)_2(HL)_2(NO_3)_2(OH)_2]\cdot 2(NO_3)$ (3). The complex **3** was prepared in the same way as **1** except that $Er(NO_3)_3\cdot 6H_2O$ (0.3 mmol, 0.124 g) was used instead of $Nd(NO_3)_3\cdot 6H_2O$ (0.3 mmol, 0.117 g). For **3**: Yield: 0.113 g, 61%. Anal. Calc. for $C_{88}H_{100}N_{12}O_{30}Er_4$: C, 42.71; H, 4.07; N, 6.79%; found: C, 42.58; H, 4.17; N, 6.76%. IR (KBr, cm^{-1}): 3414 (b), 3066 (w), 2940 (m), 2860 (w), 1652 (s), 1618 (m), 1558 (m), 1504 (m), 1469 (vs), 1383 (m), 1357 (w), 1288 (s), 1240 (w), 1227 (s), 1169 (m), 1146 (w), 1100 (w), 1078 (m), 1060 (w), 1043 (w), 1025 (w), 964 (w), 949 (w), 903 (w), 844 (m), 783 (w), 740 (m), 695 (w), 659 (w), 611 (w), 561 (w), 502 (w), 481 (w), 443 (w). ESI-MS (in MeCN) *m/z*: 2412.86 (100%), $[M - NO_3]^+$; 1175.43 (40%), $[M - (NO_3)_2]^{2+}$; 776.63 (3%), $[M - (NO_3)_3 + (MeCN)]^{3+}$ and 577.24 (17%), $[M - (NO_3)_4 + (MeCN)_2]^{4+}$; ESI-MS (in MeOH) *m/z*: 2412.86 (100%), $[M - NO_3]^+$; 1175.43 (42%), $[M - (NO_3)_2]^{2+}$; 773.63 (5%), $[M - (NO_3)_3 + (MeOH)]^{3+}$ and 572.73 (15%), $[M - (NO_3)_4 + (MeOH)_2]^{4+}$.

Synthesis of $[Gd_4(L)_2(HL)_2(NO_3)_2(OH)_2]\cdot 2(NO_3)$ (4). The complex **4** was prepared in the same way as **1** except that $Gd(NO_3)_3\cdot 6H_2O$ (0.3 mmol, 0.121 g) was used instead of $Nd(NO_3)_3\cdot 6H_2O$ (0.3 mmol, 0.117 g). For **4**: Yield: 0.117 g, 64%. Anal. Calc. for $C_{88}H_{100}N_{12}O_{30}Gd_4$: C, 43.41; H, 4.14; N, 6.90%; found: C, 43.26; H, 4.25; N, 6.85%. IR (KBr, cm^{-1}): 3414 (b), 3065 (w), 2938 (m), 2860 (w), 1651 (s), 1617 (m), 1556 (m), 1504 (m), 1457 (vs), 1384 (m), 1365 (w), 1289 (s), 1243 (w), 1224 (s), 1170 (m), 1144 (w), 1098 (w), 1075 (m), 1058 (w), 1044 (w), 1023 (w), 961 (w), 947 (w), 903 (w), 855 (m), 782 (w), 740 (m), 692 (w), 660 (w), 608 (w), 560 (w), 498 (w), 477 (w), 434 (w). ESI-MS (in MeCN) *m/z*: 2372.82 (100%), $[M - NO_3]^+$; 1155.41 (39%), $[M - (NO_3)_2]^{2+}$; 763.29 (7%), $[M - (NO_3)_3 + (MeCN)]^{3+}$ and 567.23 (13%), $[M - (NO_3)_4 + (MeCN)_2]^{4+}$; ESI-MS (in MeOH) *m/z*: 2372.82 (100%), $[M - NO_3]^+$; 1155.41 (43%), $[M - (NO_3)_2]^{2+}$; 760.28 (5%), $[M - (NO_3)_3 + (MeOH)]^{3+}$ and 562.75 (15%), $[M - (NO_3)_4 + (MeOH)_2]^{4+}$.

X-ray crystallography

Single crystals of $[Nd_4(L)_2(HL)_2(NO_3)_2(OH)_2]\cdot 2(NO_3)\cdot 3H_2O$ ($\mathbf{1}\cdot 3H_2O$), $[Yb_4(L)_2(HL)_2(NO_3)_2(OH)_2]\cdot 2(NO_3)\cdot 3H_2O$ ($\mathbf{2}\cdot 3H_2O$) and $[Er_4(L)_2(HL)_2(NO_3)_2(OH)_2]\cdot 2(NO_3)\cdot 3H_2O$ ($\mathbf{3}\cdot 3H_2O$) of suitable dimensions were mounted onto thin glass fibers. All the intensity data were collected on a Bruker SMART CCD diffractometer (Mo-Kα radiation and $\lambda = 0.71073$ Å) in Φ and ω scan modes. Structures were solved by direct methods followed by difference Fourier syntheses, and then refined by full-matrix least-squares techniques against F^2 using SHELXL-97.[17] All other non-hydrogen atoms were refined with anisotropic thermal parameters. Absorption corrections were applied using SADABS.[18] Hydrogen atoms were placed in calculated positions and refined isotropically using a riding model. In each of complexes **1–3**, the three water solvates are disordered with each O atom occupying two sets of positions, and the H atoms are not added. Crystallographic data and refinement parameters for the complexes are presented in Table 1. CCDC reference number 854306–854308 for $\mathbf{1}\cdot 3H_2O$, $\mathbf{2}\cdot 3H_2O$ and $\mathbf{3}\cdot 3H_2O$, respectively.

3. Results and discussion

Synthesis and characterization

From reaction of the deprotonated $\mathbf{L}^{2-}$ and equimolar amount of $Ln(NO_3)_3\cdot 6H_2O$ (Ln = Nd, Yb, Er or Gd) in MeOH–MeCN, series of four homoleptic $[Ln_4(L)_2(HL)_2(NO_3)_2(OH)_2]\cdot 2(NO_3)$ complexes (Ln = Nd, **1**; Ln = Yb, **2**; Ln = Er, **3**; Ln = Gd, **4**) are obtained. Similar to the good solubility of the Salen-type Schiff-base ligand $\mathbf{H_2L}$ in common organic solvents except for water, the four complexes **1–4** are also soluble in absolute MeCN or MeOH, which should be due to the use of the Salen-type Schiff-base ligand $\mathbf{H_2L}$ with the flexible linker and the charge of the two components ($[Ln_4(L)_2(HL)_2(NO_3)_2(OH)_2]^{2+}$ and NO_3^-) in each of the four complexes.

The series of four complexes **1–4** were well characterized by EA, FT-IR, ^{1}H NMR and ESI-MS. In the FT-IR spectra, the characteristic strong absorptions of the ν(C=N) vibration at 1648–1653 cm^{-1} for complexes **1–4**, are slightly blue-shifted by the range of 29–34 cm^{-1} relative to that of the free Salen-type Schiff-base ligand $\mathbf{H_2L}$ (1619 cm^{-1}) upon coordination of the Ln^{3+} ions. The two additional strong characteristic absorptions at 1452–1476 cm^{-1} and 1283–1291 cm^{-1} for the series of complexes **1–4** were observed, which are tentatively attributed to $\nu(NO_3^-)$. As to the room temperature ^{1}H NMR spectrum in CD_3CN of complex **1**, large shifts (δ from 14.58 to −5.68 ppm and 14.17 to −2.90 ppm) of two sets of the proton resonances of the $\mathbf{L}^{2-}$ ligands endowed from the observed $\mathbf{(L)}^{2-}$ and $\mathbf{(HL)}^-$ modes in the molecular structure are observed due to the Nd^{3+}-induced shift, significantly spread in relation to those of the free $\mathbf{H_2L}$ ligand (δ from 13.84 to 1.58 ppm). The ESI-MS spectra of the series of four complexes (**1–4**) in MeCN or MeOH display similar patterns and exhibit two strong mass peaks assigned to the major species $\{[Ln_4(L)_2(HL)_2(NO_3)_2(OH)_2]\cdot NO_3\}^+$ and $[Ln_4(L)_2(HL)_2(NO_3)_2(OH)_2]^{2+}$, and two fragments to $[Ln_4(L)_2(HL)_2(NO_3)(OH)_2(S)]^{3+}$ and $[Ln_4(L)_2(HL)_2(OH)_2(S)_2]^{4+}$ (S = MeCN or MeOH) for complexes **1–4**, respectively. These observations further indicate that the discrete homoleptic tetranuclear unit retains in the respective dilute MeCN or MeOH solution.

X-ray quality crystals of $\mathbf{1}\cdot 3H_2O$, $\mathbf{2}\cdot 3H_2O$ or $\mathbf{3}\cdot 3H_2O$ of the series of four complexes **1–4** were obtained, and the table of selected crystal properties are given in Table 1. For complex

Table 1 Crystal data and refinement for complexes **1**·3H_2O, **2**·3H_2O and **3**·3H_2O

Compound	**1**·3H_2O	**2**·3H_2O	**3**·3H_2O
Empirical formula	$C_{88}H_{106}N_{12}O_{33}Nd_4$	$C_{88}H_{106}N_{12}O_{33}Yb_4$	$C_{90}H_{106}N_{12}O_{33}Er_4$
Formula weight	2436.81	2552.01	2528.89
Crystal system	Triclinic	Triclinic	Triclinic
Space group	$P\bar{1}$	$P\bar{1}$	$P\bar{1}$
a/Å	14.4121(9)	14.4240(12)	14.4573(13)
b/Å	14.7205(9)	14.4630(11)	14.5690(13)
c/Å	14.7927(10)	14.633(2)	14.707(2)
α (°)	110.087(2)	111.254(2)	111.567(2)
β (°)	104.020(2)	104.137(2)	102.880(2)
γ (°)	108.7390(10)	107.6990(10)	107.5400(10)
V/Å^3	2562.5(3)	2485.0(4)	2544.9(5)
Z	1	1	1
ρ/g cm^{-3}	1.579	1.705	1.650
Crystal size/mm	0.32 × 0.27 × 0.23	0.33 × 0.26 × 0.22	0.30 × 0.26 × 0.24
μ(Mo-Kα)/mm^{-1}	2.076	3.814	3.347
Data/restraints/parameters	8717/1/619	8624/1/618	8852/1/618
Quality-of-fit indicator	1.095	1.044	1.020
Final R indices [$I > 2\sigma(I)$]	$R_1 = 0.0752$ w$R_2 = 0.1978$	$R_1 = 0.0390$ w$R_2 = 0.0956$	$R_1 = 0.0394$ w$R_2 = 0.0990$
R indices (all data)	$R_1 = 0.1150$ w$R_2 = 0.2431$	$R_1 = 0.0532$ w$R_2 = 0.1044$	$R_1 = 0.0576$ w$R_2 = 0.1114$

1·3H_2O, the structural unit is composed of one cation $[Nd_4(L)_2(HL)_2(NO_3)_2(OH)_2]^{2+}$, two free NO_3^- anions, and three solvate H_2O molecules. As shown in Fig. 1, for the cationic $[Nd_4(L)_2(HL)_2(NO_3)_2(OH)_2]^{2+}$ part lying about an inversion centre, two equivalent $Nd_2L(HL)$ moieties are bridged by two μ-O phenoxide atoms (O6 and O6a) of two Salen-type Schiff-base **(HL)**$^-$ ligands with O_4 tetradentate mode (as shown in Scheme 1) and two O atoms (O9 and O9a) of two coordinated μ_3-OH^- groups, resulting in the formation of a homoleptic cyclic tetranuclear (Nd_4(Salen)$_4$) host structure. In each of two equivalent $Nd_2L(HL)$ moieties, two Nd^{3+} (Nd1 and Nd2) ions with different

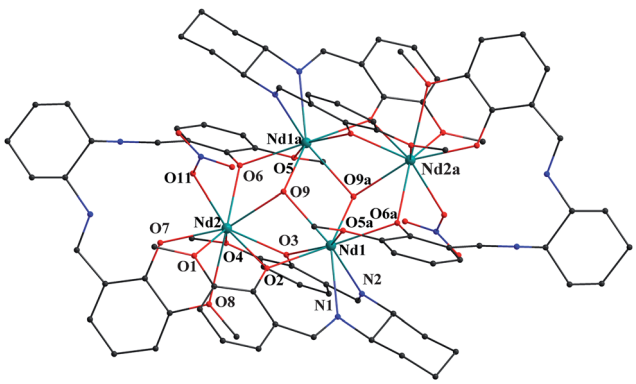

Fig. 1 Perspective drawing of the cationic part in complex **1**·3H_2O; free anions, H atoms and solvates are omitted for clarity. Selected bond length (Å) and angles (°): Nd1–N1, 2.553(9); Nd1–N2, 2.477(8); Nd1–O2, 2.382(6); Nd1–O3, 2.434(6); Nd1–O5a, 2.569(7); Nd1–O6a, 2.437(7); Nd1–O9, 2.414(7); Nd1–O9a, 2.419(6); Nd2–O1, 2.706(7); Nd2–O2, 2.441(6); Nd2–O3, 2.433(6); Nd2–O4, 2.712(7); Nd2–O6, 2.526(7); Nd2–O7, 2.361(7); Nd2–O8, 2.653(8); Nd2–O9, 2.445(6) and Nd2–O11, 2.489(9). Nd1···Nd2, 3.6407(10); Nd1···Nd2a, 3.9781(8); Nd1···Nd1a, 3.8757(11) and Nd2···Nd1a, 3.9782(8). N1–Nd1–N2, 64.2(3); O2–Nd1–O3, 68.2(2); O1–Nd2–O4, 140.2(2); O2–Nd2–O3, 67.3(2); O7–Nd2–O8, 63.0 (2) and O9–Nd2–O6, 68.7(2). Symmetry transformation used to generate equivalent atoms: a: $-x + 1$, $-y + 2$, $-z + 1$.

coordination environments are also linked by two μ-O phenoxide atoms (O2 and O3) of one Salen-type Schiff-base **(L)**$^{2-}$ ligand with N_2O_4 hexadentate mode and one O atom (O9) of the coordinated μ_3-OH^- group. The unique inner Nd^{3+} ion (Nd1) is eight-coordinate and bound by the N_2O_2 core of the Salen-type Schiff-base **(L)**$^{2-}$ ligand in addition to two O atom (O5a of MeO– group and O6a of μ-O phenoxide atom) from the Salen-type Schiff-base **(HL)**$^-$ ligand and two O atoms of two coordinated μ_3-OH^- groups. Meanwhile the outer Nd^{3+} ion (Nd2) is nine-coordinate; in addition to the seven oxygen atoms from the two outer O_2O_2 moieties of the two Salen-type Schiff-base ligands, where four O atoms (two of MeO– groups and two of phenoxide atoms) are from the Salen-type Schiff-base **(L)**$^{2-}$ ligand and three O atoms (one of MeO– groups and two of phenoxide atoms) from the Salen-type Schiff-base **(HL)**$^-$ ligand, it completes its coordination environment with one O atom from the monodentate NO_3^- anion and one O atom from the coordinated μ_3-OH^- group. The unique Nd···Nd distances are different, with the distances of 3.6407(10) and 3.8757(11)–3.9782(8) Å for Nd1···Nd2, Nd1···Nd1a and Nd2···Nd1a, respectively, in which each of the Nd1···Nd2 separations in the equivalent $Nd_2L(HL)$ moieties is slightly shorter than that (Nd1···Nd1a or Nd2···Nd1a separation) between two equivalent $Nd_2L(HL)$ moieties. For the inner Nd^{3+} ion (Nd1 or Nd1a), the Nd–O bond length (2.414(7)–2.419(6) Å; O atoms from coordinated μ_3-OH^- group) or the Nd–N bond lengths (2.477(8)–2.553(9) Å) are in the range of the Nd–O bond lengths (2.382(6)–2.569(7) Å) with O atoms from the phenoxo groups. For the outer Nd^{3+} ion (Nd2 or Nd2a), the nine Nd–O bond lengths also depend on the nature of the oxygen atoms, varying from 2.361(7) to 2.712(7) Å, in which the bond lengths (2.653(8)–2.712(7) Å) from the oxygen atoms of MeO– groups are distinctively longer than those (2.361(7)–2.526(7) Å or 2.489(9) Å and 2.445(6) Å) from the phenoxo oxygen atoms, monodentate NO_3^- anion or coordinated μ_3-OH^- group. It is interesting to note the presence of an "apical" triply bridged μ_3-OH^- group for each of the two central O atoms (O9 or O9a), which could be shown from the reasonable directionality of the

interactions with three Nd^{3+} ions. Furthermore, as to the cationic $[Nd_4(L)_2(HL)_2(NO_3)_2(OH)_2]^{2+}$ part, the charge should be balanced by the protonation of one (N4 or N4a) of the imino nitrogen atoms for two of the four deprotonated Salen-type Schiff-base $\mathbf{(L)^{2-}}$ ligands, which endows the formation of two strong intramolecular H-bond interactions with the short N4–H4···O7 distance (2.575(17) Å) shown in Fig. 1s.† The three solvate H_2O molecules and the two free NO_3^- anions of complex $\mathbf{1}\cdot 3H_2O$ are not bound to the framework and they exhibit no observed interactions with the host structure.

It is worth noting that the homoleptic cyclic tetranuclear ($Nd_4(Salen)_4$) host structure in complex $\mathbf{1}\cdot 3H_2O$ is distinctively different from the reported structures of binuclear triple-decker,[11] trinuclear triple-decker,[12] trinuclear tetra-decker[13] or pentanuclear tetra-decker lanthanide complexes[14] based on the Salen-type Schiff-base ligands with the rigid linkers, which should be due to the use of the flexible Salen-type Schiff-base ligand $\mathbf{H_2L}$ with the outer O_2O_2 moiety for complex $\mathbf{1}\cdot 3H_2O$. On the other hand, the formation of homoleptic cyclic tetranuclear ($Nd_4(Salen)_4$) framework in complex $\mathbf{1}\cdot 3H_2O$ appears to be NO_3^- anion-dependent since the use of other LnX_3 ($X^- = OAc^-$ or $CF_3SO_3^-$) in the self-assembly with the Salen-type Schiff-base ligands with the flexible linkers usually results in the formation of polymeric lanthanide coordination complexes.[15] It is of special interest to compare the self-assembly of complex $\mathbf{1}\cdot 3H_2O$ with that of the reported $Tb_4(Salen)_6$ complex.[16] Although the similar tetranuclear framework is obtained necessarily from the Salen-type Schiff-base ligands with flexible linkers, the character of the Salen-type Schiff-base ligand $\mathbf{H_2L}$ with both the inner N_2O_2 core and the outer O_2O_2 moiety in complex $\mathbf{1}\cdot 3H_2O$, instead of the pure Salen-type Schiff-base ligand without the outer O_2O_2 moiety in the reported $Tb_4(Salen)_6$ complex[16] endows the unusual formation of NO_3^- anion-dependent homoleptic cyclic tetranuclear ($Nd_4(Salen)_4$) framework in complex $\mathbf{1}\cdot 3H_2O$. Single-crystal X-ray diffraction analyses indicated that both complex $\mathbf{2}\cdot 3H_2O$ and $\mathbf{3}\cdot 3H_2O$ are isomorphous with complex $\mathbf{1}\cdot 3H_2O$, as shown in Fig. 2 and 3, and the similar strong intramolecular H-bond interactions with the short N4–H4···O7 distances (2.605(11) Å for $\mathbf{2}\cdot 3H_2O$ and 2.602(11) Å for $\mathbf{3}\cdot 3H_2O$) are observed in Fig. 2s and 3s,† respectively. The effect of lanthanide contraction causes the slight variation of the detailed structures.

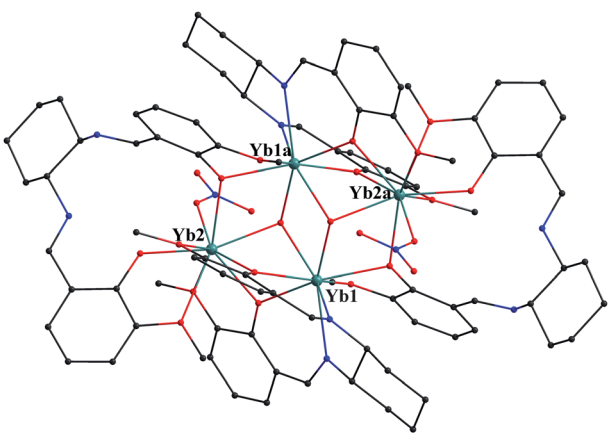

Fig. 2 Perspective drawing of the cationic part in complex $\mathbf{2}\cdot 3H_2O$; free anions, H atoms and solvates are omitted for clarity.

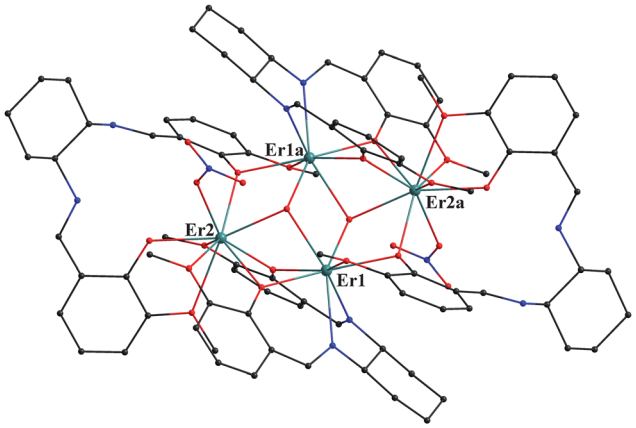

Fig. 3 Perspective drawing of the cationic part in complex $\mathbf{3}\cdot 3H_2O$; free anions, H atoms and solvates are omitted for clarity.

Photophysical properties

The photophysical properties of the ligand $\mathbf{H_2L}$ and complexes **1–4** have been examined in dilute MeCN solution at room temperature or 77 K, and summarized in Table 2 and Fig. 4–6. As shown in Fig. 4, the similar ligand-centered solution absorption spectra (225–227, 267–268 and 339–342 nm) of complexes **1–4** in the UV-visible region are observed and are red-shifted upon the coordination of the Ln^{3+} ions as compared to that (221, 259 and 332 nm) of the ligand $\mathbf{H_2L}$ or $\mathbf{(L)^{2-}}$ in MeCN or in MeOH (shown in Fig. 4s†). The molar absorption coefficients of complexes **1–4** in all the lowest energy bands are almost four orders of magnitude larger than that of the ligand $\mathbf{H_2L}$ due to the involvement of four chromophores. For complexes **1–3**, the similar residual visible emission bands (*ca.* 505 nm and $\tau < 1$ ns, almost undetectable) and low quantum yields ($\Phi_{em} < 10^{-5}$) in dilute absolute MeCN solution at room temperature are observed. While photoexcitation of the antennae at the range of 230–500 nm ($\lambda_{ex} = 402$ nm for **1** or 385 nm for **2**), as shown in Fig. 5, gives rise to the characteristic emissions of the Nd^{3+} ion ($^4F_{3/2} \rightarrow {}^4I_{J/2}$, $J = 9, 11, 13$) and the Yb^{3+} ion ($^2F_{5/2} \rightarrow {}^2F_{7/2}$) in the NIR region. For complex **1**, the emissions at 909, 1085 and 1365 nm can be respectively assigned to $^4F_{3/2} \rightarrow {}^4I_{9/2}$, $^4F_{3/2} \rightarrow {}^4I_{11/2}$ and $^4F_{3/2} \rightarrow {}^4I_{13/2}$ transitions of the Nd^{3+} ion, and the emission at 1022 nm can be attributed to the $^2F_{5/2} \rightarrow {}^2F_{7/2}$ transition of the Yb^{3+} ion for complex **2**. Moreover, unlike complex **1** or **2**, the characteristic NIR emission of the Er^{3+} ion for complex **3** is too weak to be detected. The ligand $\mathbf{H_2L}$ or the complex **4** also does not exhibit the NIR luminescence under the same conditions, and just have the typical luminescence ($\lambda_{em} = 361$, $\tau = 1.21$ ns and $\phi = 0.23 \times 10^{-3}$; $\lambda_{em} = 479$ nm, $\tau = 1.56$ ns and $\phi = 0.25 \times 10^{-3}$ for the ligand $\mathbf{H_2L}$ or $\lambda_{em} = 505$ nm, $\tau = 0.74$ ns and $\phi = 0.64 \times 10^{-3}$ for **4**) of the Salen-type Schiff-base ligand in the visible region, as shown in Fig. 6. It is worth noting that for complex **1** or **2**, the similar excitation spectrum ($\lambda_{ex} = 385$ and 403 nm for **1** or $\lambda_{ex} = 402$ nm for **2**) monitored at the respective strongest NIR emission peak ($\lambda_{em} = 1085$ nm for **1** or $\lambda_{em} = 1022$ nm for **2**) or the visible emission peak ($\lambda_{em} = 505$ nm) of

Table 2 The photophysical properties of the H_2L and complexes **1–4** at 1×10^{-5} M in absolute MeCN solution at room temperature or 77 K

Compound	Absorption λ_{ab}/nm (log[ε/dm^3 mol^{-1} cm^{-1}])	Excitation λ_{ex}/nm	Emission λ_{em}/nm (τ, $\Phi \times 10^3$)
H_2L	221 (0.24), 259 (0.11), 332 (0.03)	303, 321, 370	361 (1.21 ns, 0.23), 479 (1.56 ns, 0.25)
1	227 (0.74), 268 (0.31), 342 (0.11)	385, 403(sh)	909 (1.39 μs), 1085 (s, 1.41 μs), 1365[a]
2	225 (0.76), 268 (0.33), 339 (0.11)	307(sh), 357, 402(sh)	1022 (13.22 μs)
3	226 (0.82), 267 (0.35), 339 (0.12)	—[b]	—[b]
4	226 (0.83), 267 (0.35), 339 (0.12)	290(sh), 350, 397	505 (0.74 ns, 0.64) 487 (2.4 ns, 77 K), 543 (6.2 ms, 77 K)

[a] Due to the limitations of the instrument, we were unable to measure the lifetime of the NIR luminescence above 1300 nm. [b] The emission is too weak to be detected.

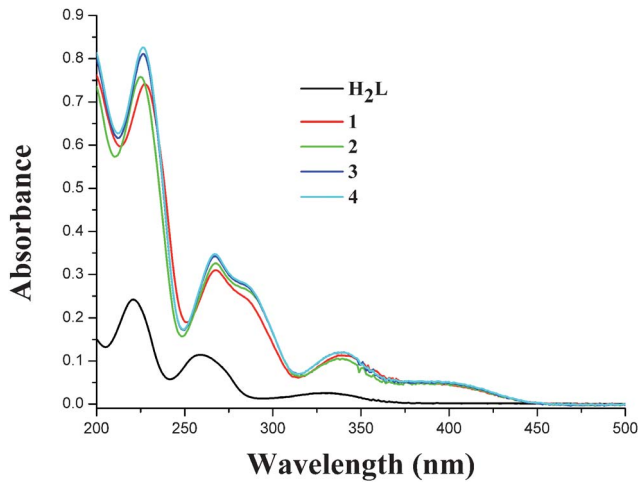

Fig. 4 UV-Vis spectra of the ligand H_2L and complexes **1–4** in MeCN solution at 1×10^{-5} M at room temperature.

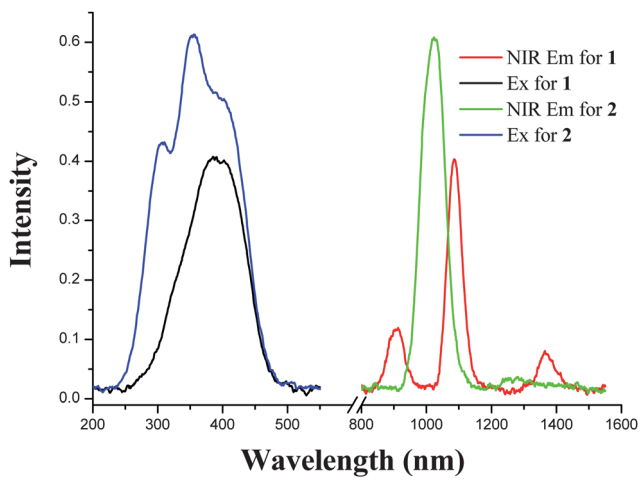

Fig. 5 NIR emission and excitation spectra of complexes **1** and **2** in MeCN solution at 1×10^{-5} M at room temperature.

complex **4**, clearly show both the NIR emissions originate from the same π–π* transitions of the H_2L Schiff-base ligand for complexes **1** and **2**, suggests that the energy transfer from the antenna to the Ln^{3+} ions takes place efficiently.[19] Moreover, for complexes **1** and **2**, the respective NIR luminescent decay curves

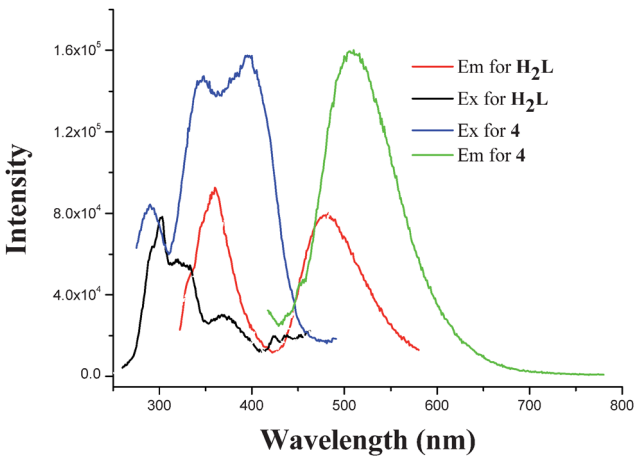

Fig. 6 Visible emission and excitation spectra of the ligand H_2L and complex **4** in MeCN solution at 1×10^{-5} M at room temperature.

obtained from time-resolved luminescent experiments can be fitted mono-exponentially with time constant of microseconds (1.41 μs for **1** at 1085 nm and 13.22 μs for **2** at 1022 nm), and the intrinsic quantum yield Φ_{Ln} (0.564% for **1** or 0.661% for **2**) of the Ln^{3+} emission may be estimated by $\Phi_{Ln} = \tau_{obs}/\tau_0$, where τ_{obs} is the observed emission lifetime and τ_0 is the "natural lifetime", *viz* 0.25 ms and 2.0 ms for the Nd^{3+} and Yb^{3+} ions, respectively,[20] The relatively smaller NIR intrinsic quantum yields of complexes **1** and **2** compared with those of trinuclear triple-decker[12] or pentanuclear tetra-decker lanthanide (Nd^{3+} or Yb^{3+}) complexes[14] based on the Salen-type Schiff-base ligand with the rigid linker should be as a result of the partially luminescent quenching effect by the OH-vibrators from coordinated μ_3-OH^- groups around the Ln^{3+} ions, in spite of the involvement of more chromophores.

As a reference compound, complex **4** allows the further study of the antennae luminescence in the absence of energy transfer, because the Gd^{3+} ion has no energy levels below 32 000 cm^{-1}, and therefore cannot accept any energy from the antennae excited state.[21] In dilute MeCN solution at 77 K, complex **4** displays the strengthened antennae fluorescence compared with that (λ_{em} = 505 nm, τ = 0.74 ns and $\phi = 0.65 \times 10^{-3}$) at room temperature under the same conditions, which shows higher luminescent intensity (λ_{em} = 487 nm and 543 nm) and distinctively longer luminescence lifetimes (2.4 ns and 6.2 ms). This result shows that the sensitization of the NIR luminescence for complexes **1–2** should arise from both the ^{1}LC (20534 cm^{-1}) and the ^{3}LC (18416

cm^{-1}) excited state of the Schiff-base ligand **H_2L** at low temperature. If the antennae luminescence lifetime of complex **4** is to represent the excited-state lifetime in the absence of the energy transfer, the energy transfer rate (k_{ET}) in the complexes **1** and **2** can thus be calculated from $k_{ET} = 1/\tau_q - 1/\tau_u$,[22] where τ_q is the residual lifetime of the luminescent emission undergoing quenching by the respective Ln^{3+} ion, and τ_u is the unquenched lifetime in the reference complex **4**, so the energy transfer rates for the Nd^{3+} and Yb^{3+} ions in complexes **1** and **2** may all be estimated to be above 5×10^8 s^{-1}, which could well imply the reason for the effective energy transfer for complexes **1** and **2**. Furthermore, from the viewpoint of the energy level match, in spite of the effective energy transfer also taking place in complex **3**, the larger energy gap between the energy-donating ^{3}LC level (18 416 cm^{-1}) and the emitting level ($^4I_{13/2}$) of Er^{3+} ion than those of complexes **1** and **2** results in the great non-radiative energy loss during the energy transfer, which should be the reason for the weak and unobservable luminescence in the range of 800–1800 nm for complex **3**.[23] As to the relatively higher quantum efficiency of **2** (0.661%) than that of **1** (0.564%), besides the smaller energy gap ($^2F_{5/2}$, 9785 cm^{-1}) of Yb^{3+} ion in complex **2** than that ($^4F_{3/2}$, 9217 cm^{-1}) of the Nd^{3+} ion in complex **1**, the excited state of the Nd^{3+} ion in complex **1** is more sensitive to quenching by the distant C–H or N–H oscillators of the Salen-type Schiff-base ligand **H_2L** and the O–H oscillators of the coordinated μ_3-OH^- groups around the Ln^{3+} ions.[24] Furthermore, the sensitivity of the NIR luminescent intensities to different solvents for complexes **1** and **2** becomes apparent when the determined solvent is changed from MeCN to CD_3CN or CD_3OD. In CD_3CN or CD_3OD, the typical emission bands of Nd^{3+} ion assigned to the $4F_{3/2} \rightarrow 4I_{J/2}$ ($J = 9$, 11 or 13) transitions for complex **1** and the emission band of Yb^{3+} ion attributed to the $^2F_{5/2} \rightarrow 2F_{7/2}$ transition for complex **2** are also observed, which indicates that the two complexes with the discrete homoleptic tetranuclear units can be stabilized in different solvents (MeCN or MeOH), consistent with those found from the results of ESI-MS. Moreover, for either complex **1** or **2**, the relative strongest emission intensities (*ca.* 1085 nm for complex **1** and *ca.* 1022 nm for complex **2**) in CD_3CN and CD_3OD are higher (almost 1.8 times for **1** and 1.5 times for **2** in CD_3CN; 2.6 times for **1** and 3.7 times for **2** in CD_3OD) than those for the two complexes in MeCN when using solutions with their concentrations adjusted to give the same absorbance values at *ca.* 276 nm. The observed changes following the deuteration of solvents may be relative to an interaction of the solvents (MeCN or MeOH from the dissociated fragments with the loss of coordinated NO_3^- anions shown in ESI-MS data) with the Ln^{3+} ions.[9d]

4. Conclusion

Through the self-assembly of the flexible hexadentate Salen-type Schiff-base ligand **H_2L** with $Ln(NO_3)_3 \cdot 6H_2O$ (Ln = Nd, Yb, Er or Gd), series of homoleptic cyclic tetranuclear $[Ln_4(L)_2(HL)_2(NO_3)_2(OH)_2] \cdot 2(NO_3)$ (Ln = Nd, **1**; Ln = Yb, **2**; Ln = Er, **3**; Ln = Gd, **4**) are obtained under similar reaction conditions. The results of their photophysical studies show that more Salen-type Schiff-base ligands may work as antennae or chromophores for the sensitization of NIR luminescence of Nd^{3+} and Yb^{3+} ions, and the characteristic NIR luminescence with emissive lifetimes in the microsecond range, arises from the excited state (both ^{1}LC and ^{3}LC) of the ligand due to the effective intramolecular energy transfer in complexes **1** and **2**. Moreover, the energy level match between the excited states (^{3}LC) of the chromophores to the corresponding Ln^{3+} ion's exciting state is required for the enhancement of NIR luminescence, in addition to avoiding or decreasing the luminescent quenching effect arising from OH-, CH– or NH-oscillators around the Ln^{3+} ion. The specific design of polynuclear complexes from the flexible Salen-type Schiff-base ligands in facilitating the NIR sensitization is now under way.

Acknowledgements

This work is funded by the National Natural Science Foundation (21173165, 20871098), the Program for New Century Excellent Talents in University from the Ministry of Education of China (NCET-10-0936), the Research Fund for the Doctoral Program (20116101110003) of Higher Education of China, the State Key Laboratory of Structure Chemistry (20100014), the Education Committee Foundation of Shaanxi Province (11JK0588), Hong Kong Research Grants Council (HKBU 202407 and FRG/06-07/II-16) in P. R. of China, the Robert A. Welch Foundation (Grant F-816), the Texas Higher Education Coordinating Board (ARP 003658-0010-2006) and the Petroleum Research Fund, administered by the American Chemical Society (47014-AC5).

References

1 (*a*) J. Kido and Y. Okamoto, *Chem. Rev.*, 2002, **102**, 2357; (*b*) J.-C. G. Bünzli and C. Piguet, *Chem. Soc. Rev.*, 2005, **34**, 1048; (*c*) J.-C. G. Bünzli and S. V. Eliseeva, *J. Rare Earths*, 2010, **28**, 824; (*d*) J.-C. G. Bünzli, *Chem. Rev.*, 2010, **110**, 2729.
2 (*a*) M. P. Hogerheide, J. Boersma and G. V. Konten, *Coord. Chem. Rev.*, 1996, **155**, 87; (*b*) S. Tanase and J. Reedijk, *Coord. Chem. Rev.*, 2006, **250**, 2501.
3 (*a*) S. Comby and J.-C. G. Bünzli, in *Handbook on the Physics and Chemistry of Rare Earths*, ed. K. A. Gschneidner Jr, J.-C. Bünzli and V. K. Pecharsky, Elsevier Science B.V., Amsterdam, 2007, vol. 37, ch. 235; (*b*) T. Nishioka, K. Fukui and K. Matsumoto, in *Handbook on the Physics and Chemistry of Rare Earths*, ed. K. A. Gschneidner Jr, J.-C. Bünzli and V. K. Pecharsky, Elsevier Science B.V., Amsterdam, 2007, vol. 37.
4 (*a*) P. A. Vigato and S. Tamburini, *Coord. Chem. Rev.*, 2008, **252**, 1871; (*b*) X.-J. Zhu, W.-K. Wong, W.-Y. Wong and X.-P. Yang, *Eur. J. Inorg. Chem.*, 2011, 4651; (*c*) J. Jankolovits, C. M. Andolina, J. W. Kampf, K. N. Raymond and V. L. Pecoraro, *Angew. Chem., Int. Ed.*, 2011, **50**, 9660.
5 (*a*) H. Tsukube, Y. Suzuki, D. Sykes, Y. Kataoka and S. Shinoda, *Chem. Commun.*, 2007, 2533; (*b*) W.-Q. Fan, J. Feng, S.-Y. Song, Y.-Q. Lei, L. Zhou, G.-L. Zheng, S. Dang, S. Wang and H.-J. Zhang, *Nanoscale*, 2010, **2**, 2096.
6 X.-P. Yang, R. A. Jones, M. M. Oye, M. Wiester and R. J. Lai, *New J. Chem.*, 2011, **35**, 310.
7 S. V. Eliseeva and J.-C. G. Bünzli, *Chem. Soc. Rev.*, 2010, **39**, 189.
8 L. Winkless, R. H. C. Tan, Y. Zheng, M. Motevalli, P. B. Wyatt and W. P. Gillin, *Appl. Phys. Lett.*, 2006, **89**, 111115.
9 (*a*) W.-K. Wong, H.-Z. Liang, W.-Y. Wong, Z.-W. Cai, K.-F. Li and K.-W. Cheah, *New J. Chem.*, 2002, **26**, 275; (*b*) W.-K. Lo, W.-K. Wong, J.-P. Guo, W.-Y. Wong, K.-F. Li and K.-W. Cheah, *Inorg. Chim. Acta*, 2004, **357**, 4510; (*c*) W.-K. Lo, W.-K. Wong, W.-Y. Wong, J.-P. Guo, K.-T. Yeung, Y.-K. Cheng, X.-P. Yang and R. A. Jones, *Inorg. Chem.*, 2006, **45**, 9315; (*d*) W.-K. Wong, X.-P. Yang, R. A. Jones, J. H. Rivers, V. Lynch, W.-K. Lo, D. Xiao, M. M. Oye and A. L. Holmes, *Inorg. Chem.*, 2006, **45**, 4340; (*e*) X.-P. Yang, R. A. Jones, W.-K. Wong, M. M. Oye and A. L. Holmes, *Chem. Commun.*, 2006, 1836; (*f*) W.-Y. Bi, X.-Q. Lü, W.-L. Chai, J.-R. Song, W.-K. Wong, X.-P. Yang and R. A. Jones,

Z. Anorg. Allg. Chem., 2008, **634**, 1795; (*g*) X.-Q. Lü, W.-Y. Bi, W.-L. Chai, J.-R. Song, J.-X. Meng, W.-Y. Wong, W.-K. Wong and R. A. Jones, *New J. Chem.*, 2008, **32**, 127; (*h*) S.-S. Zhao, X.-Q. Lü, A.-X. Hou, W.-Y. Wong, W.-K. Wong, X.-P. Yang and R. A. Jones, *Dalton Trans.*, 2009, 9595; (*i*) W.-Y. Bi, T. Wei, X.-Q. Lü, Y.-N. Hui, J.-R. Song, W.-K. Wong and R. A. Jones, *New J. Chem.*, 2009, **33**, 2326; (*j*) X.-Q. Lü, W.-Y. Bi, W.-L. Chai, J.-R. Song, J.-X. Meng, W.-Y. Wong, W.-K. Wong, X.-P. Yang and R. A. Jones, *Polyhedron*, 2009, **28**, 27; (*k*) X.-Q. Lü, W.-X. Feng, Y.-N. Hui, T. Wei, J.-R. Song, S.-S. Zhao, W.-Y. Wong, W.-K. Wong and R. A. Jones, *Eur. J. Inorg. Chem.*, 2010, 2714.

10 (*a*) K. N. Dutt and K. Nag, *J. Inorg. Nucl. Chem.*, 1968, **30**, 2493; (*b*) J.-P. Costes, J.-P. Laussac and F. Nicodème, *J. Chem. Soc., Dalton Trans.*, 2002, 2731.

11 P.-F. Yang, S. Chen, J.-W. Zhang and G.-M. Li, *CrystEngComm*, 2011, **13**, 36.

12 X.-P. Yang, R. A. Jones, M. M. Oye, A. L. Holmes and W.-K. Wong, *Cryst. Growth Des.*, 2006, **6**, 2122.

13 X.-P. Yang and R. A. Jones, *J. Am. Chem. Soc.*, 2005, **127**, 7686.

14 X.-P. Yang, R. A. Jones and W.-K. Wong, *Dalton Trans.*, 2008, 1676.

15 (*a*) W. Xie, M. J. Heeg and P. G. Wang, *Inorg. Chem.*, 1999, **38**, 2541; (*b*) X.-P. Yang, R. A. Jones, J. H. Rivers and W.-K. Wong, *Dalton Trans.*, 2009, 10505; (*c*) X.-P. Yang, D. Lam, C. Chan, J. M. Stanley, R. A. Jones, B. J. Holliday and W.-K. Wong, *Dalton Trans.*, 2011, **40**, 9795.

16 X.-P. Yang, R. A. Jones and W.-K. Wong, *Chem. Commun.*, 2008, 3266.

17 G. M. Sheldrick, *SHELXL-97, Program for solution of crystal structures*, University of Göttingen, Germany, 1997.

18 G. M. Sheldrick, *SADABS, Program for area detector adsorption correction*, Institute for Inorganic Chemistry, University of Göttingen, Germany, 1996.

19 M. Albrecht, O. Osetska, J. Klankermayer, R. Fröhlich, F. Gumy and J.-C.-G. Bünzli, *Chem. Commun.*, 2007, 1834.

20 (*a*) M. J. Weber, *Phys. Rev.*, 1968, **171**, 283; (*b*) M. L. Mercyri, P. Deplano, L. Pilia, A. Serpe and F. Artizzu, *Coord. Chem. Rev.*, 2010, **254**, 1419.

21 W. T. Carnall, P. R. Fields and K. Rajnak, *J. Chem. Phys.*, 1968, **49**, 4443.

22 D. L. Dexter, *J. Chem. Phys.*, 1953, **21**, 836.

23 J.-C. G. Bünzli, S. Comby, A.-S. Chauvin and C. D. B. Vandevyver, *J. Rare Earths*, 2007, **25**, 257.

24 A. Beeby, I. M. Clarkson, R. S. Dockins, S. Faulkner, D. Parker, L. Royle, A. S. de Souda, J. A. G. Williams and M. Woods, *J. Chem. Soc., Perkin Trans.*, 1999, **2**, 493.